Synthesis and multicolor emission properties of polystyrene with difluoroboron avobenzone complexes at side chains

Synthesis and multicolor emission properties of polystyrene with difluoroboron avobenzone complexes at side chains

Katsuya Shimizu, Arisa Okuma, Shiho Katsumi, Fuyuki Ito,

Seiya Kobatake

Manuscript for publication to *Dyes. Pigm.* as a Regular Article

Synthesis and Multicolor Emission Properties of Polystyrene with Difluoroboron Avobenzone Complexes at Side Chains

Katsuya Shimizu,[a] Arisa Okuma,[b] Shiho Katsumi,[b], Fuyuki Ito,[b,*] Seiya Kobatake[a,*]

[a]*Department of Applied Chemistry, Graduate School of Engineering, Osaka City University, 3-3-138 Sugimoto, Sumiyoshi-ku, Osaka, 558-8585, Japan*
[b]*Department of Chemistry, Institute of Education, Shinshu University, 6-ro Nishinagano, Nagano, 380-8544, Japan*

*Corresponding author.
E-mail address: kobatake@a-chem.eng.osaka-cu.ac.jp (S. Kobatake)
E-mail address: fito@shinshu-u.ac.jp (F. Ito)

Keywords: Solid emission; BF_2 complex; Polymerization, Avobenzone; White emission

ABSTRACT:

Random copolymers (poly(ABSt-*co*-St)) consisting of avobenzone-BF_2 complex monomer (ABSt) and styrene (St) were synthesized and used for emission color tuning including white-like emission in the solid state using St units as a spacer. The emission color of ABSt in the resulting copolymers changed from green to blue via bluish-white by changing the content of St. The fluorescence quantum yields of the polymers in the solid state were relatively high (Φ_f = 0.30–0.51) independent of the composition contents. The polymers have two main emission bands around 440 and 540 nm, which were derived from the emission of single-molecule and amorphous aggregation, respectively. The fluorescence color changed according to a change in the ratio of the fluorescence intensity at 440 and 540 nm (F_{440}/F_{540}). The absorption and fluorescence properties of the polymers in tetrahydrofuran were independent of the composition ratio of ABSt and St, which indicates no intermolecular interaction between avobenzone-BF_2 (AB) fluorophores in the intra-polymer chain. The emission color of all polymers in the solution was blue and the fluorescence spectra were the same as that of ABSt in the solution. Thus, emission color changes observed in the solid state were mainly derived from the intermolecular interaction between AB fluorophores in inter-polymer chains because the polymers intertwined each other in the solid state. When the polymers in the solid state were annealed, F_{440}/F_{540} increased and all of the fluorescence spectra became similar to that of monomer emission according to the arrangement change of the polymer chain. It is concluded that emission color changes of the polymers are mainly derived from intermolecular interaction between AB fluorophores in the inter-polymer chains. We have demonstrated that poly(ABSt-*co*-St) forms excellent homogeneous fluorescence polymer films. In contrast, the mixture of methoxy AB (ABOMe) and poly(St) undergoes crystallization even in the low content of ABOMe in poly(St).

1. Introduction

In recent years, a luminescent molecule exhibiting a change in the emission property in response to the concentration and the environment has attracted much attention in terms of application for sensing materials [1–5]. For instance, pyrene derivatives are known to form the excimer derived from high planarity of the molecule in concentrated state and emit the fluorescence in a longer wavelength region [5–10]. The fluorophore with high planarity and small Stokes-shift such as boron dipyrromethene (BODIPY) derivatives also exhibits emission from green to red by self-quenching and dimer formation [11–16]. Difluoroboron Avobenzone (AB) complexes are known to be emissive in solid state and exhibit mechanochromism upon mechanical stimuli such as grinding and striking [17–24]. It is reported that a mechanochromic property is caused by the change in the molecular arrangement and the phase transition from a crystalline state to an amorphous state. Ito and coworkers revealed the assembly process of AB in the course of evaporation of the solution using spectroscopic and image analysis [20]. The process could be explained by a two-step nucleation model from the solution state via the amorphous state to the crystalline phase. Ikeda and co-workers have also reported the effect of the substituent and the packing pattern for various AB derivatives to the fluorescent properties [25,26]. Chujo and co-workers have focused on boron-containing polymers because of excellent properties such as high charge carrier mobilities, prominent optical properties, high stability, and high processability. Especially, they reported emission color tuning and brightness of polymers containing boron complexes such as boron-diketonate or diiminate at the main chains and side chains [27–30].

In these days, the preparation for white emissive material has attracted because of potential applications for lighting devices and display media [25–35]. In general, to produce white emission, it is necessary to combine three primary RGB (red, green and blue) colors or at least two complementary colors with proper composition ratios. If white emission could be achieved by using a single fluorophore, then the materials would be promising for practical application. To date, several approaches for white emission using a single fluorophore were reported [36–39]. However, single-molecular white emission is still quite rare, and it is still worth challenging to create a white-emitting material consisting of a single fluorophore.

Here, we have focused on dual emission which is blue (monomer) and yellowish-green (amorphous) of AB and the possibility of white emission by combining their phases in an appropriate feed ratio. However, AB sometimes crystallizes even in polymers because of high crystallinity by high planarity of the Avobenzone moiety. In this work, we report on the design and fabrication of random copolymers (poly(ABSt-*co*-St)) consisting of AB monomer (ABSt) and styrene (St) to achieve multicolor and white emission in the solid state using St as a spacer as shown in Fig. 1. The optical properties of poly(ABSt-*co*-St) in various media such as solutions, bulk powder, and bulk film are also discussed in this paper.

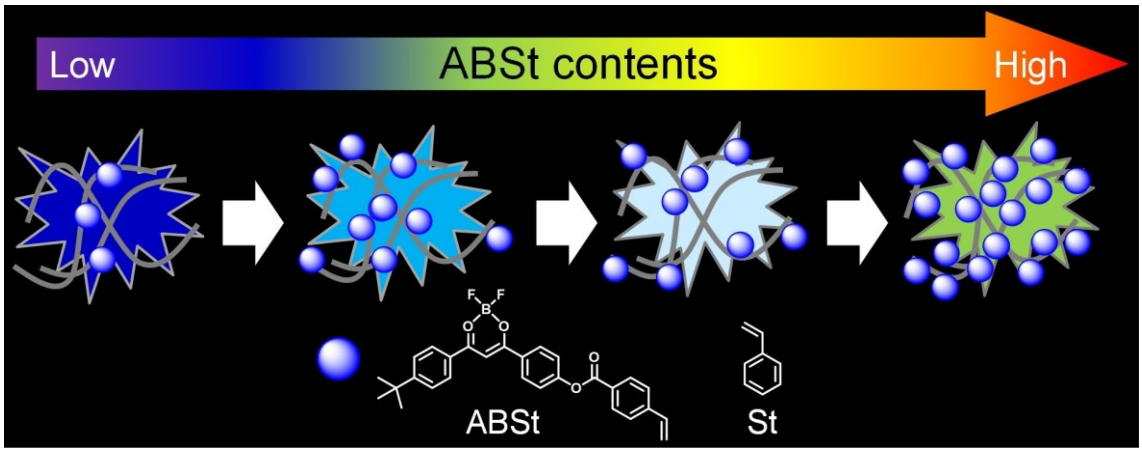

Fig. 1. Emission color changes of copolymers consisting of ABSt and St with different composition contents.

2. Experimental Section

2.1. Measurements

Spectroscopic grade solvents used were purified by distillation before use. ^{1}H NMR (300 MHz) and ^{13}C NMR (75 MHz) spectra were recorded on a BRUKER AV-300N spectrometer using tetramethylsilane (TMS) as an internal standard. Infrared (IR) spectra were recorded on a JASCO FT/IR-4100 spectrometer. Mass spectra were obtained using a Bruker FT-ICR/solariX mass spectrometer. Elemental analysis was performed using J-SCIENCE LAB JM10 CHN Analyzer Micro Corder. Differential scanning calorimetry (DSC) was run using a HITACHI DSC-7000X. Absorption spectra were measured with a JASCO V-560 absorption spectrophotometer. Fluorescence spectra were measured with a JASCO FP-8300 fluorescence spectrometer. Fluorescence quantum yields were also determined with the fluorescence spectrometer equipped with a JASCO ILF-835 integrate sphere. Recycling preparative high-performance liquid chromatography (HPLC) was conducted using a JAI LC-908 chromatograph equipped with JAIGEL-1H and 2H columns using chloroform as the eluent. Gel-permeation chromatography (GPC) was performed using a TOSOH 8000 series GPC system equipped with TSK-gel columns and tetrahydrofuran (THF) as the eluent at 40 °C. CIE coordinates were measured using a HAMAMATSU PMA-11. Fluorescence microscopic images were taken by OLYMPUS IX71. Fluorescence spectra in the local area were obtained using a hyperspectral camera of EBA JAPAN SI108. Every pixel in the hyperspectral digital image contains a continuous spectrum.

2.2. Materials

All reagents were commercially available from FUJIFILM Wako Pure Chemical Corporation. 2,2'-Azobis(isobutyronitrile) (AIBN) was recrystallized from methanol. Difluoroboron-1-(*p*-*t*-butylphenyl)-3-(*p*-methoxyphenyl)-1,3-propanedione (ABOMe) was prepared according to a method described in literature [17].

2.3. Synthesis of Avobenzone having styryl group (ASt)

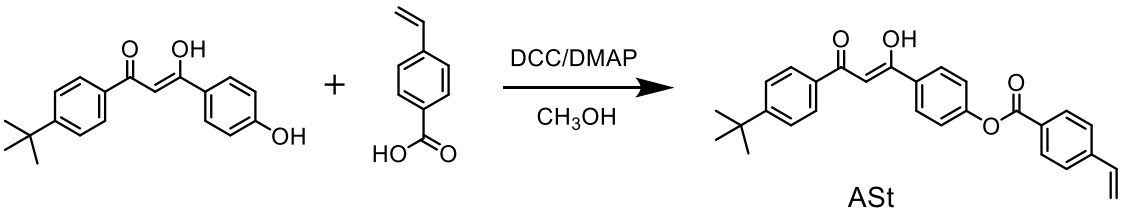

ASt

1-(*p*-*t*-Butylphenyl)-3-(*p*-hydroxyphenyl)-1,3-propanedione (0.67 g, 2.3 mmol) was dissolved in methanol (80 mL). 4-Dimethylaminopyridine (DMAP) (0.33 g, 2.7 mmol), *p*-vinylbenzoic acid (0.44 g, 2.7 mmol) and dicyclohexylcarbodiimide (DCC) (0.56 g, 2.7 mmol) were added to the solution and stirred for 18 h at room temperature. The reaction mixture was extracted with chloroform. The organic layer was dried over $MgSO_4$, filtered, and concentrated in vacuo. The crude product was purified by column chromatography on silica gel using chloroform as the eluent to give 0.35 g of 1-(*p*-*t*-butylphenyl)-3-(*p*-vinylbenzoyloxyphenyl)-1,3-propanedione (ASt) in 36% yield. The ^{1}H NMR, ^{13}C NMR, and IR spectra of the product are shown in Fig. S1.

^{1}H NMR (300 MHz, $CDCl_3$, TMS) δ = 1.35 (s, 9H, $C(CH_3)_3$), 5.45 (d, *J* = 10.8 Hz, 1H, Vinyl H), 5.93 (d, *J* = 17.8 Hz, 1H, Vinyl H), 6.80 (dd, *J* = 10.8 Hz, 17.8 Hz, 1H, Vinyl H), 6.84 (s, 1H, CO−C**H**=C−OH), 7.36 (d, *J* = 8.7 Hz, 2H, Aromatic H), 7.50-7.56 (m, 4H, Aromatic H), 7.94 (d, *J* = 8.3 Hz, 2H, Aromatic H), 8.07 (d, *J* = 8.7 Hz, 2H, Aromatic H), 8.17 (d, *J* = 8.3 Hz, 2H, Aromatic H). ^{13}C NMR (75 MHz, $CDCl_3$, TMS) δ = 31.3, 35.2, 93.0, 117.3, 122.2, 125.8, 126.5, 127.2, 128.3, 128.8, 130.7, 132.8, 133.5, 136.0, 143.0, 154.3, 156.5, 164.6, 184.7, 185.8. IR (*v*, KBr, cm^{-1}): 1603, 1732, 2590, 2867, 2958, 3068, 3447. HR-MS (MALDI) *m*/*z* = 427.1904 (M^+). Calcd for $C_{28}H_{26}O_4^+$: 427.1904.

2.4. Synthesis of ABSt

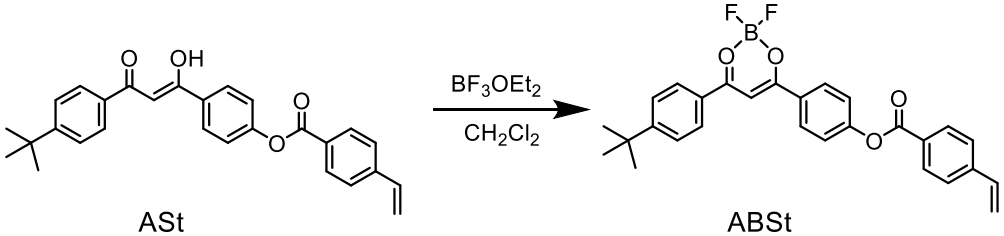

ASt ABSt

Trifluoroborate etherate (0.50 mL, 22 mmol) was added to the solution of dichloromethane (50 mL) dissolving ASt (0.32 g, 0.75 mmol). Then, the reaction mixture was stirred for 4 h at

45 °C. The reaction mixture was concentrated in vacuo. The crude product was purified by column chromatography on silica gel using *n*-hexane/ethyl acetate (7:3) as the eluent to give 0.20 g of ABSt in 56% yield. ABSt was purified by recrystallization from dichloromethane: mp = 218 °C. The ^{1}H NMR, ^{13}C NMR, and IR spectra of the product are shown in Fig. S2.

^{1}H NMR (300 MHz, $CDCl_3$, TMS) δ = 1.38 (s, 9H, $C(CH_3)_3$), 5.47 (d, *J* = 11.0 Hz, 1H, Vinyl H), 5.94 (d, *J* = 17.6 Hz, 1H, Vinyl H), 6.81 (dd, *J* = 11.0 Hz, 17.6 Hz, 1H, Vinyl H), 7.17 (s, 1H, CO−C**H**=C−O), 7.46 (d, *J* = 8.9 Hz, 2H, Aromatic H), 7.52-760 (m, 4H, Aromatic H), 8.11 (d, *J* = 8.7 Hz, 2H, Aromatic H), 8.17 (d, *J* = 8.7 Hz, 2H, Aromatic H), 8.24 (d, *J* = 8.9 Hz, 2H, Aromatic H). ^{13}C NMR (75 MHz, $CDCl_3$, TMS) δ = 31.1, 35.7, 93.2, 117.6, 122.7, 126.4, 126.6, 127.9, 129.2, 129.3, 129.7, 130.6, 130.8, 135.9, 143.3, 156.5, 160.1, 164.2, 181.5, 183.4. IR (*v*, KBr, cm^{-1}): 1546, 1603, 1738, 2867, 2905, 2965, 3090, 3161. HR-MS (MALDI) *m*/*z* = 455.1822 ($(M - F)^+$). Calcd for $C_{28}H_{25}BFO_4^+$: 455.1824. Anal. Calcd. for $C_{28}H_{25}BF_2O_4$: C, 70.90; H, 5.31; N, 0.00. Found: C, 70.62; H, 5.50; N, 0.00.

2.5. Polymerization

Radical copolymerization of ABSt and St was conducted in a glass tube sealed under vacuum. The monomers, AIBN, and toluene were placed in a glass tube. The tube was degassed by several freeze-pump-thaw cycles and sealed under vacuum. After polymerization for a prescribed time at 60 °C, the polymers were isolated by separation using a recycling preparative HPLC.

3. Results and discussion

3.1. Optical properties of ABSt in solution and solid state

Fundamental optical properties of ABSt such as UV-Vis. absorption spectrum including molar extinction coefficient (ε) and fluorescence spectrum were measured at a concentration of 1×10^{-5} M in THF as shown in Fig. S3. ABSt has a maximum absorption wavelength at 374 nm and high ε (55700 M^{-1} cm^{-1}) at the wavelength. Two main emission bands at 407 and 427 nm and high fluorescence quantum yield ($\Phi_f = 0.66$) were observed. Moreover, the dependence of emission properties on the concentration of ABSt in THF was examined to reveal the optical properties without any intermolecular interaction. Fig. 2 shows fluorescence spectra and optical images for ABSt at concentrations of 10^{-6} to 10^{-2} M excited with 365 nm light. Table 1 summarizes these results. Regardless of the concentration, the shapes of fluorescence spectra were almost similar. However, the spectra were slightly red-shifted and the ratio of fluorescence intensity for two main bands (F_{409}/F_{427}) decreased at a higher concentration. The fluorescence quantum yield also decreased with increasing concentration. These optical property changes are possibly caused by self-quenching between ABSt fluorophores because of small overlapping of absorption and fluorescence spectra. This case is similar to that of BODIPY monomer we previously reported [11].

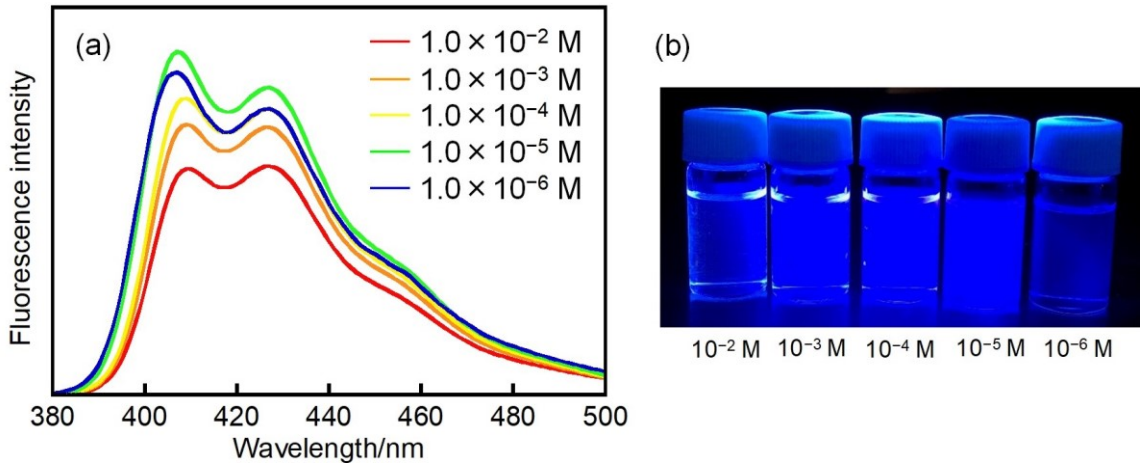

Fig. 2. (a) Fluorescence spectra and (b) optical image of ABSt in THF. The fluorescence spectra were recorded under excitation with 365 nm light. Optical images were also taken under illumination with 365 nm light.

Table 1

Fluorescence properties of ABSt at various concentrations in THF.

[ABSt]/M	λ_{em}/nm	F_{409}/F_{427}	Φ_f
1×10^{-2}	409, 427	0.989	0.44
1×10^{-3}	409, 427	1.011	0.52
1×10^{-4}	409, 427	1.039	0.57
1×10^{-5}	407, 427	1.124	0.66
1×10^{-6}	407, 427	1.127	0.62

The optical properties of ABSt in solid state were investigated. Fig. 3 shows fluorescence spectra and images of ABSt in THF, the crystalline state, and the amorphous state illuminated with 365 nm light. The results are summarized in Table 2. The amorphous sample was prepared by heating the crystal at more than the melting point followed by cooling rapidly at room temperature. At the initial crystalline state, the emission band is sharp and located around 450 nm (pale blue emission). After melting the crystal, the emission spectrum was significantly red-shifted and located around 540 nm (green emission) followed by a slight increase in Φ_f. The changes in CIE coordinate in three states are shown in Fig. 4(c).

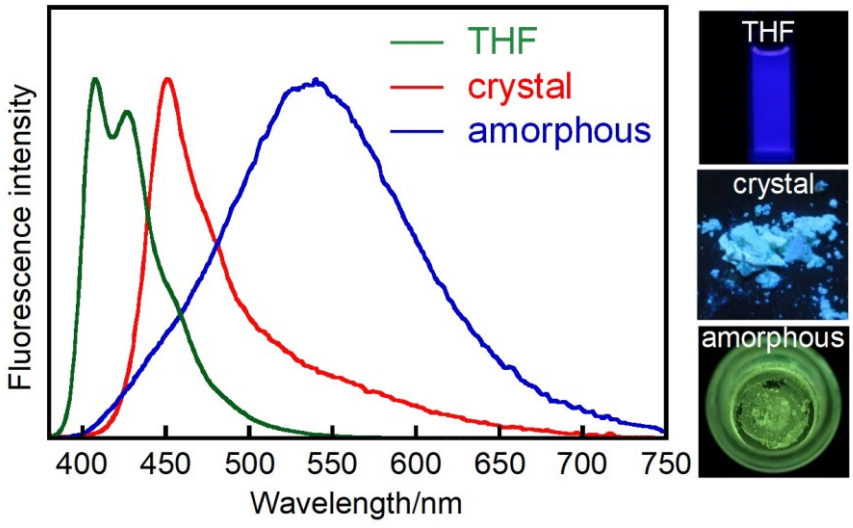

Fig. 3. Fluorescence spectra and images of ABSt in THF (1.8×10^{-6} M), the crystalline state, and the amorphous state illuminated with 365 nm light.

Table 2

Optical properties of ABSt in different media illuminated with 365 nm light.

	λ_{em}/nm	Φ_f	CIE
THF[a)]	408, 426	0.61	(0.15, 0.06)
Crystal	451	0.04	(0.20, 0.25)
Amorphous	540	0.09	(0.32, 0.54)

a) [ABSt] = 1.8×10^{-6} M

3.2. Synthesis and characterization of poly(ABSt-co-St)

Poly(ABSt-*co*-St)s with various contents of ABSt and St were prepared to control the intermolecular interaction of ABSt and achieve the multicolor emission using St as a spacer (Entries 1–6). Random copolymerization of ABSt and St was conducted using AIBN as an initiator in toluene at 60 °C for 10 h, as shown in Scheme 1. After the polymerization, the polymers were isolated by recycling preparative HPLC and frozen-dried in benzene in order to get powder samples. The unreacted ABSt monomer and St were completely removed by this method. Table 3 summarizes the polymerization condition and results such as reaction yield, M_n, M_w/M_n, and composition ratios of ABSt and St in the resultant polymers. GPC elution curves are also shown in Fig. S4. The copolymer compositions were determined by ^{1}H-NMR spectroscopic analysis of aromatic protons for ABSt and St, as shown in Figs. S5–S10. The peaks around 7.4–8.4 ppm were assigned to the phenyl protons in ABSt moiety as indicated by e, f, g, i, and j. The peaks at 6.2–6.8 ppm correspond to *o*-protons of the phenyl group in the styryl groups in ABSt and St as indicated by d and p. The peaks at 6.8–7.2 ppm correspond to the *m*- and *p*-protons of the phenyl group in St as indicated by q and the proton of CO−C**H**=C−O in ABSt as indicated by h. Therefore, the copolymer compositions of ABSt for Entries 1–6 were estimated to be 2.44–0.23 mol%, as shown in Table 3. These results indicate that various contents of poly(ABSt-*co*-St) were successfully synthesized and the composition contents of ABSt decreased with increasing content of St. We also calculated the number of ABSt and St in a single polymer chain using M_n and the composition contents. The resulting polymer hardly includes ABSt fluorophore in single polymer chains, indicating that the ABSt fluorophores can exist in isolation not only in solution but also in the polymer chain. DSC chart of the polymer

indicates that the polymer has a glass transition temperature (T_g) of 104 °C corresponding to that of poly(St), as shown in Fig. S11. It also means that the ABSt fluorophore exists in isolation in the polymer chain.

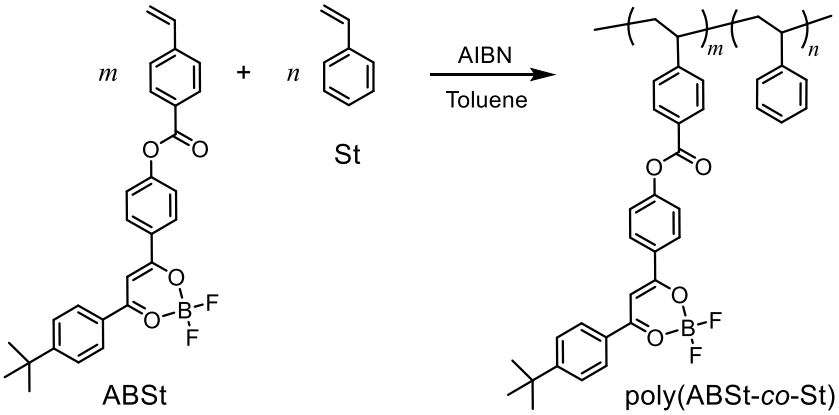

Scheme 1. Synthetic scheme of poly(ABSt-*co*-St)

Table 3

Copolymerization of ABSt and St in toluene at 60 °C for 10 h.

Entry	[ABSt] /M	[St] /M	[St]/[ABSt]	[AIBN] /M	Yield /%	M_n (GPC)	M_w/M_n (GPC)	Composition ratio of ABSt in copolymer /mol%	In a polymer chain	
									m	*n*
1	0.03	3.0	100	0.02	32	20700	1.66	2.44	4.5	180
2	0.017	3.0	170	0.02	26	21700	1.72	0.99	2.0	200
3	0.015	3.0	200	0.02	17	10000	1.70	0.83	0.8	96
4	0.012	3.0	250	0.02	45	16000	1.54	0.66	1.0	150
5	0.006	3.0	500	0.02	32	16500	1.64	0.34	0.5	160
6	0.003	3.0	1000	0.02	35	21000	1.64	0.23	0.5	220

3.3. Optical properties of poly(ABSt-co-St) in bulk powder and THF

The optical properties of poly(ABSt-*co*-St) in bulk powder were investigated. Fig. 4 shows the fluorescence spectra, optical images, and CIE coordinates of poly(ABSt-*co*-St) with various contents of ABSt and St. Table 4 summarizes the maximum fluorescence wavelength, Φ_f, and CIE coordinates. The emission color of the resulting copolymers changed from blue to green via bluish-white with the change in the content of ABSt from 0.23 (Entry 6) to 2.44 mol% (Entry 1), accompanying a change in CIE coordinates from (0.18, 0.13) to (0.31, 0.44). In the

process of the emission color changes, the fluorescence spectra changed with the change in the ratio of the fluorescence intensities at 440 and 540 nm (F_{440}/F_{540}). For poly(ABSt-*co*-St) (Entry 1), the main band was around 530 nm which is ascribed to the fluorescence of ABSt in the amorphous state. The environment of ABSt in polymer chains became to single-molecule isolated by a lot of St units. Thus, the main band in fluorescence spectra became to be around 440 nm for Entries 2–6. The fluorescence quantum yields of the polymers in the solid state were relatively high (Φ_f = 0.30–0.51) independent of the composition contents. It is remarkable that poly(ABSt-*co*-St) (Entry 2) exhibited a bright emission (Φ_f = 0.46) and the CIE (0.27, 0.35) which is close to pure white color (0.33, 0.33), which was brought by the just good combination of blue and green emission. However, the red component should be added into this system of ABSt and St to achieve the pure white emission.

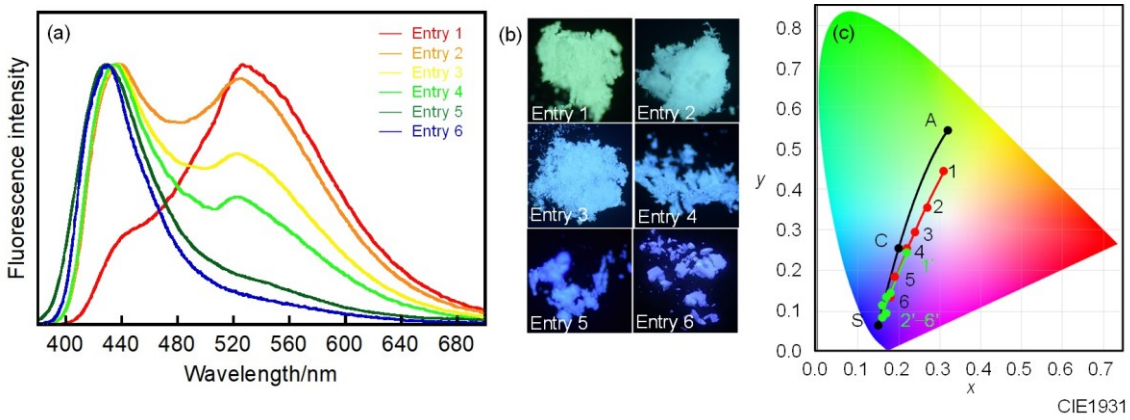

Fig. 4. (a) Fluorescence spectra of poly(ABSt-*co*-St) in bulk powder excited with 365 nm light, (b) optical images of poly(ABSt-*co*-St) illuminated with 365 nm light, and (c) CIE chromaticity diagram of ABSt and poly(ABSt-*co*-St) in bulk powder (1–6) and bulk film (1′–6′).

Here, the emission color changes are caused by intermolecular interaction between ABSt fluorophores in inter- or intra-polymer chains. To elucidate the main factor affecting the emission color changes of poly(ABSt-*co*-St), the optical properties of poly(ABSt-*co*-St) in solution were also examined. Fig. 5 shows absorption and fluorescence spectra of poly(ABSt-*co*-St) in THF. The optical properties are summarized in Table 4. The shapes of the spectra were very similar to that of ABSt, which indicates that intermolecular interaction between ABSt

fluorophores in the same polymer chain is small because the polymers behave as single polymer chains without any aggregation in solution. All of Φ_f were also similar to that of ABSt in THF.

To get further evidence for the change in emission color, the poly(ABSt-*co*-St) powders were annealed at 200 °C followed by cooling to measure the fluorescence spectra. Fig. S12 shows fluorescence spectra of poly(ABSt-*co*-St) before and after annealing. The results are summarized in Table 4. The ratio of fluorescence intensity F_{440}/F_{540} relative to the molar ratio [St]/[ABSt] before and after annealing were also shown in Fig. S13. Overall, F_{440}/F_{540} increased by annealing, indicating that the environment of ABSt in a polymer chain becomes similar to that in solution. In other words, the intermolecular distance between ABSt fluorophores was increased by annealing and cooling of polymers. Nevertheless, it is surprising that almost Φ_f somehow decreased after annealing. Taking these results into consideration, it is concluded that the emission color changes of the copolymers were mainly caused by intermolecular interaction between ABSt fluorophores in the inter-polymer chains.

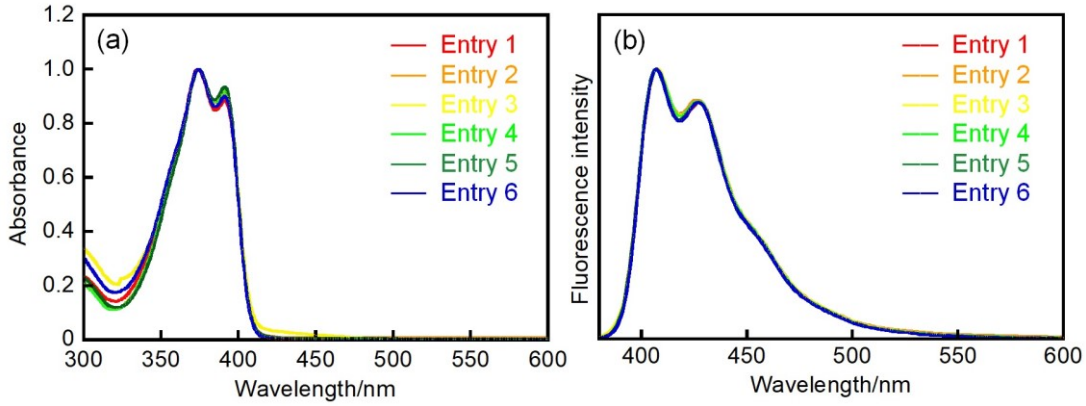

Fig. 5. (a) Absorption and (b) fluorescence spectra of poly(ABSt-*co*-St) in THF excited with 365 nm light.

Table 4

Optical properties of poly(ABSt-*co*-St)

entry	In bulk powder before annealing			In bulk powder after annealing		In THF		In bulk film		
	λ_{em}/nm	Φ_f	CIE	λ_{em}/nm	Φ_f	λ_{em}/nm	Φ_f	λ_{em}/nm	Φ_f	CIE
1	527	0.30	(0.31, 0.44)	526	0.35	407, 428	0.59	438	0.16	(0.22, 0.24)
2	439, 525	0.46	(0.27, 0.35)	438,	0.45	407, 426	0.68	432	0.35	(0.17, 0.13)
3	437, 522	0.34	(0.24, 0.29)	435,	0.25	408, 427	0.57	431	0.51	(0.16, 0.11)
4	434	0.47	(0.22, 0.25)	432	0.35	407, 427	0.61	433	0.68	(0.18, 0.14)
5	430	0.51	(0.19, 0.18)	431	0.53	407, 427	0.61	430	0.47	(0.17, 0.09)
6	430	0.45	(0.18, 0.13)	431	0.27	407, 427	0.57	430	0.55	(0.16, 0.08)

3.4. Optical properties of poly(ABSt-co-St) in bulk film

The optical properties of poly(ABSt-*co*-St) in bulk film were examined in order to demonstrate the advantage of using these materials as bulk powders. Fig. 6 shows fluorescence spectra and optical images of poly(ABSt-*co*-St) in bulk film excited with 365 nm light. The maximum fluorescence wavelength and Φ_f are summarized in Table 4. Fig. 4(c) also shows CIE coordinates of poly(ABSt-*co*-St) with various contents of ABSt and St in bulk film. The film samples were prepared by drop-casting onto a glass plate and drying a THF solution dissolving poly(ABSt-*co*-St). Overall, the band at longer wavelength decreased and the band around 440 nm increased compared with the case of bulk powder. For the polymers (Entries 4, 5, and 6), the optical properties and the shapes of fluorescence spectra were very similar between bulk powder and film. In the process of dissolution and drying, the level of isolating of ABSt fluorophores possibly did not change because the number of St against ABSt is very high. However, compared with the case of bulk powder, the style of emission spectral changes among each sample in bulk film is very different from each other and the difference in emission color is not so significant. Taking these results into consideration, it is difficult to achieve multi-color emission with a bulk film because of the difficulty of controlling the intermolecular distance between ABSt fluorophores.

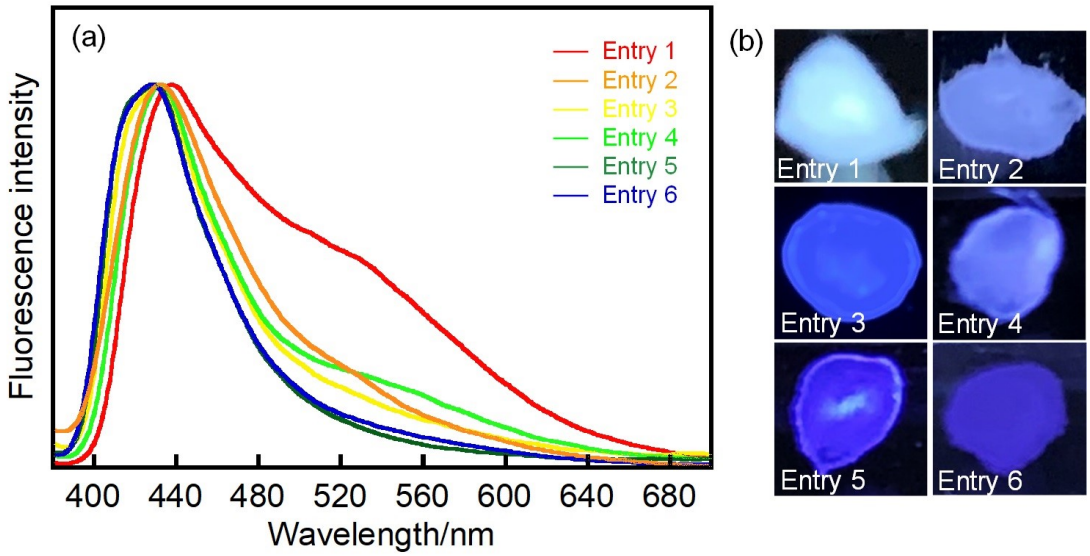

Fig. 6. (a) Fluorescence spectra and (b) optical images of poly(ABSt-*co*-St) in bulk film excited with 365 nm light.

3.5. Optical properties for mixtures of ABOMe and poly(St) (ABOMe/poly(St))

Two kinds of polymer films with different contents of ABOMe in poly(St) were prepared and the emission properties were examined. ABOMe/poly(St) including 2.4 mol% and 1.0 mol% of ABOMe which is the same as the composition contents of poly(ABSt-*co*-St) (Entries 1 and 2) were prepared by drop-casting of the ABOMe/poly(St) solution in 1,2-dichloroethane followed by drying. Figs. S14 and S15 show fluorescence color images during evaporation under illumination with 365 nm light. Regarding ABOMe/poly(St) (2.4 mol%), blue emission was observed in early in evaporation. And then, the area exhibiting green emission derived from the amorphous state was gradually increased. Finally, light blue emission derived from the crystalline phase appeared in the edge area, whereas the area at the central part still remained green emission. On the other hand, for ABOMe/poly(St) (1.0 mol%), blue emission was also observed in early in evaporation. After the complete evaporation of the solvent, light blue emission appeared at the edge area and blue emission was observed in the amorphous state at the central part. Fig. 7 shows fluorescence spectra of ABOMe/poly(St) at the central part, the edge area, and the total area using a hyperspectral camera under excitation with 365 nm light. The shoulder peaks around 450 nm increased as the crystallization proceeded in the edge area. Thus, the mixture of ABOMe and poly(St) forms heterogeneous polymer film even in low

contents of ABOMe. These results indicate that the just addition of ABOMe fluorophore into the polymer results in crystallization and it is difficult to prepare a homogeneous polymer film. Therefore, it is concluded that poly(ABSt-co-St) has an excellent advantage to form homogeneous fluorescence polymer film without any crystallization.

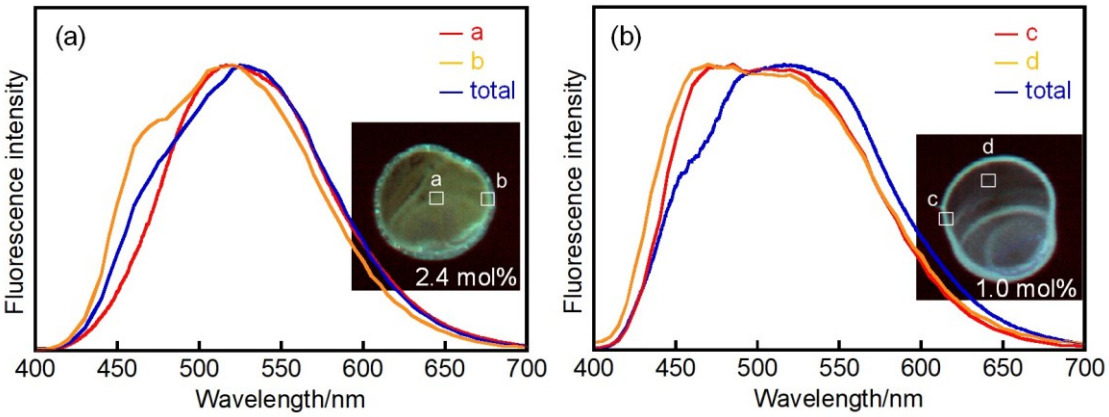

Fig. 7. (a) Fluorescence spectra of ABOMe/poly(St) (2.4 mol%) (red line: Area a, orange line: Area b, blue line: total area). (b) Fluorescence spectra of ABOMe/poly(St) (1.0 mol%) (red line: Area c, orange line: Area d, blue line: total area).

4. Conclusion

Poly(ABSt-*co*-St) was synthesized and the emission properties were investigated. Multi-color fluorescent materials with white-like emission using a single fluorophore were successfully prepared. Poly(ABSt-*co*-St) (Entry 2) exhibited a bright emission ($\Phi_f = 0.46$) and the CIE (0.27, 0.35) which is close to pure white color (0.33, 0.33). The emission color changes of the polymers were demonstrated as being caused by intermolecular interaction between the ABSt fluorophores in not an intra-polymer chain but inter-polymer chains. The possibility of multi-color emission and white emission could be spread by using mechanical responsive fluorophores.

Notes

The authors declare no competing financial interests.

Acknowledgments

This work was partly supported by JSPS KAKENHI Grant Numbers JP26107013 (S. Kobatake) and JP17H05253 (F. Ito) in Scientific Research on Innovative Areas “Photosynergetics” and JP19H02686 (F. Ito) in Scientific Research (B). The authors (K. Shimizu and S. Kobatake) also acknowledge Program for Leading Graduate Schools for System-inspired Leaders in Material Science: SiMS, Osaka Prefecture University/Osaka City University from MEXT, Japan.

References

[1] Mei J, Leung N, Kwok R, Lam J, Tan BZ, Aggregation-induced emission: together we shine, united we soar! Chem Rev 2015;115:11718–940.

[2] Ciardelli F, Ruggeri G, Pucci A, Dye-containing polymers: methods for preparation of mechanochromic materials. Chem Soc Rev 2013;42:857–70.

[3] Liu J, Guo X, Hu R, Xu J, Wang S, Li S, Li Y, Yang G, Intracellular fluorescenct temperature probe based on triarylboron substituted poly n-isopropylacrylamide and energy transfer, Anal Chem 2015;87:3694–8.

[4] Qi Y, Kang R, Huang J, Zhang W, He G, Yin S, Fang Y, Reunderstanding the fluorescent behavior of four-coordinate monoboron complexes containing monoanionic bidentate ligands. J Phys Chem B 2017;121:6189–99.

[5] Ng K, Zheng G, Molecular interaction in organic nanoparticle for phototheranostic applications. Chem Rev 2015;115:11012–42.

[6] Ito F, Kakiuchi T, Sakano T, Nagamura T, Fluorescence properties of pyrene derivative aggregates formed in polymer matrix depending on concentration. Phys Chem Chem Phys 2010;12:10923–7.

[7] Tu J, Sun S, Xu Y, A novel self-assembled platform for the ratiometric fluorescence detection of spermine. Chem Commun 2016;52:1040–3.

[8] Nohta H, Satozono H, Koiso K, Yoshida H, Ishida J, Yamaguchi M, Highly selective fluorometric determination of polyamines based on intramolecular excimer-forming derivatization with a pyrene-labeling reagent. Anal Chem 2000;72:4199–204.

[9] Yoshitake T, Yamaguchi M, Nohta H, Ichinose F, Yoshida H, Yoshitake S, Fuxe K, Kehr J, Determination of histamine in microdialysis samples from rat brain by microbore column liquid chromatography following intramolecular excimer-forming derivatization with pyrene-labeling reagent, J Neuroscience Methods 2003;127:11–7.

[10] Winnik FM, Photophysics of preassociated pyrenes in aqueous polymer solutions and in other organized media, Chem Rev 1993;93:587–614.

[11] Shimizu K, Kitagawa D, Kobatake S, Solid emission color tuning of polymers consisting of BODIPY and styrene in various ratios, Dyes Pigm 2019;161:341–6.

[12] Okada D, Nakamura T, Braam D, Dao TD, Ishii S, Nagao T, Lorke A, Nabeshima T, Yamamoto Y, Color-tunable resonant photoluminescence and cavity-mediated multistep energy transfer cascade. ACS Nano 2016;10:7058–63.

[13] Maeda C, Todaka C, Ueda T, Ema T. Color-tunable solid-state fluorescence emission from carbazole-based bodipys. Chem Eur J 2016;22:7508–13.

[14] Vu TT, Dvorko M, Schmidt EY, Audibert JF, Retailleau P, Trofimov BA, Pansu RB, Clavier G, Méallet-Renault R. Understanding the spectroscopic properties and aggregation process of a new emitting boron dipyrromethene (bodipy). J Phys Chem C 2013;117:5373–85.

[15] Bonardi L, Kanaan H, Camerel F, Jolinat P, Retailleau P, Ziessel R, Fine-tuning of yellow or red photo- and electroluminescence of functional difluoro-boradiazaindacene films. Adv Funct Mater 2008;18:401–13.

[16] Loudet A, Burgess K. Bodipy dyes and their derivatives: syntheses and spectroscopic properties. Chem Rev 2007;107:4891–932.

[17] Ito F, Kikuchi C, Concentration-dependent fluorescence color tuning of the difluoroboron avobenzone complex in polymer films, Bull Chem Soc Jpn 2017;90,709–13.

[18] Sagawa T, Ito F, Sakai A, Ogata Y, Tanaka K, Ikeda H, Substituent-dependent backward reaction in mechanofluorochromism of dibenzoylmethanatoboron difluoride derivatives, Photochem Photobio Sci 2016;15.420–30.

[19] Kosicka J, DeRosa CA, Morris WA, Fan Z, Fraser CL, Dual-emissive difluoroboron naphthyl-phenyl β-diketonate polylactide materials: effects of heavy atom placement and

polymer molecular weight, Macromolecules 2014;47:3736–46.

[20] Ito F, Suzuki Y, Fujimori J, Sagawa T, Hara M, Seki T, Yasukuni R, Chapelle M, Direct visualization of the two-step nucleation model by fluorescence color changes during evaporative crystallization from solution, Sci Rep 2019;6:22918.

[21] Louis M, Brosseau A, Guillot R, Ito F, Allain C, Métivier R, Polymorphism, Mechanofluorochromism, and Photophysical Characterization of a Carbonyl Substituted Difluoroboron-β-Diketone Derivative, J Phys Chem C 2017;121:15897–907.

[22] Wilbraham L, Louis M, Alberga D, Brosseau A, Guillot R, Ito F, Labat F, Métivier R, Allain C, Ciofini I, Adv Mater 2018;30:1800817.

[23] Louis M, García CP, Brosseau A, Allain C, Métivier R, Mechanofluorochromism of a difluoroboron-β-diketonate derivative at the nanoscale, Phys Chem Lett 2019;10:4758–62.

[24] Ito F, Saigusa M, Kanayama N, Evaporative crystallization of dibenzoylmethanato boron difluoride probed by time-resolved quartz crystal microbalance responses with fluorescence changes, Chem Lett 2019;48:1199–202.

[25] Tanaka M, Ohta E, Sakai A, Yoshimoto Y, Mizuno K, Ikeda H, Remarkable difference in fluorescence lifetimes of the crystalline states of dibenzoylmethanatoboron difluoride and its diisopropyl derivative, Tetrahedron Lett 2013;54:4380–4.

[26] Sakai A, Ohta E, Yoshimoto Y, Tanaka M, Matsui Y, Mizuno K, Ikeda H, New fluorescence domain “excited multimer” formed upon photoexcitation of continuously stacked diaroylmethanatoboron difluoride molecules with fused π-orbitals in crystals, Chem Eur J 2015;21:18128–37.

[27] Nagai A, Kokado K, Nagata Y, Chujo Y, 1,3-Diketone-based organoboron polymers: emission by extending π-conjugation along a polymeric ligand, Macromolecules 2008;41:8295–8.

[28] Yoshii R, Nagai A, Tanaka K, Chujo Y, Boron-ketoiminate-based polymers: fine-tuning of the emission color and expression of strong emission both in the solution and film states, Macromol Rapid Commun 2014;35:1315–9.

[29] Yoshii R, Hirose A, Tanaka K, Chujo Y, Functionalization of boron diiminates with unique optical properties: multicolor tuning of crystallization-induced emission and introduction

into the main chain of conjugated polymers, J Am Chem Soc 2014;136:18131–9.

[30] Tanaka K, Yanagida T, Hirose A, Yamane H, Yoshii R, Chujo Y, Synthesis and color tuning of boron diiminate conjugated polymers with aggregation-induced scintillation properties, RSC Adv 2015;5:96653–9.

[31] Reineke S, Lindner F, Schwartz G, Seidler N, Walzer K, Lüssem B, Leo K, White organic light-emitting diodes with fluorescent tube efficiency, Nature 2009;459:234–8.

[32] Gather MC, Köhnen A, Falcou A, Becker H, Meerholz K, Solution-processed full-color polymer organic light-emitting diode displays fabricated by direct photolithography, Adv Mater 2007;17:191–200.

[33] Farinola G, Ragni R, Electroluminescent materials for white light emitting diodes, Chem Soc Rev 2011;40:3467–82.

[34] Vijayakumar C, Praveen K, Ajayaghosh A, RGB emission through controlled donor self-assembly and modulation of excitation energy transfer: a novel strategy to white-light-emitting organogels, Adv Mater 2009;21:2059–63.

[35] Shinde S, Asha SK, Temperature sensitive emission color tuning and white light emission in segmented opv polymer: perylene bisimide supramolecular complex, Macromolecules 2016;49:8134–45.

[36] Wu H, Ying L, Yang W, Cao Y, Progress and perspective of polymer white light-emitting devices and materials, Chem Soc Rev 2009;38:3391–400.

[37] Furuta PT, Deng L, Garon Simona, Thompson ME, Fréchet JMJ, Platinum-functionalized random copolymers for use in solution-processible, efficient, near-white organic light-emitting diodes, J Am Chem Soc 2004;126:15388–9.

[38] Zhang M, Yin S, Zhang J, Zhou Z, Saha ML, Lu C, Stang PJ, Metallacycle-cored supramolecular assemblies with tunable fluorescence including white-light emission, PNAS 2017;114:3044–9.

[39] Malinge J, Allain C, Brosseau A, Audebert P, White fluorescence from core-shell silica nanoparticles, Angew Chem Int Ed 2012;51:8534–7.

[40] Sava DF, Pohwer LES, Rodriguez MA, Nenoff TM, Intrinsic broad-band white-light emission by a tuned, corrugated metal-organic framework, J Am Chem Soc

2012;134:3983–6.

[41] Nag A, Sarma DD, White light from Mn^{2+}-doped cds nanocrsytals: a new approach, J Phys Chem C 2007;111,37:13641–4.

[42] Wang H, Li Y, Zhang Y, Mei J, Su J, A new strategy for achieving single-molecular white-light emission: using vibration-induced emission (VIE) plus aggregation-induced emission (AIE) mechanisms as a two-pronged approach, Chem Commun 2019;55:1879–82.

[43] Li D, Hu W, Wang J, Zhang Q, Cao X-M, Ma X, Tian H, White-light emission from a single organic compound with unique self-folded conformation and multistimuli responsiveness, Chem Sci 2018;9:5709–15.

[44] Xu B, Wu H, Chen J, Yang Z, Yang Z, Wu YC, Zhang Y, Jin C, Lu PY, Chi Z, Liu S, Xu J, Aldred M, White-light emission from a single heavy atom-free molecule with room temperature phosphorescence, mechanochromism and thermochromism, Chem Sci 2017;8:1909–14.

[45] Xie Z, Chen C, Xu S, Li J, Zhang Y, Liu S, Xu J, Chi Z, White-light emission strategy of a single organic compound with aggregation-induced emission and delayed fluorescence properties, Angew Chem Int Ed 2015;54:7181–4.

Graphical Abstract